Polymer Journal

Synthesis of New Fluorene-Indolocarbazole Alternating Copolymers for Light-Emitting Diodes and Field Effect Transistors

By Wen-Ya LEE,[1] *Chien-Wei CHEN,*[2] *Chu-Chen CHUEH,*[1] *Chang-Chung YANG,*[3] *and Wen-Chang CHEN*[1,2,*]

New alternating copolymers of poly(2,7-(9,9′-dihexylfluorene)-*alt*-3,9-(5,11-di(2-ethylhexyl)-indolo[3,2-b]carbazole)) **(PF-p-In)** and poly(2,7-(9,9′-dihexylfluorene)-*alt*-2,8-(5,11-di(2-ethylhexyl)-indolo[3,2-b]carbazole)) **(PF-m-In)** were synthesized by palladium-catalyzed Suzuki coupling polymerization and characterized for the applications of light-emitting diodes and field effect transistors (FET). The incorporation of indolocarbazole into polyfluorene could not only enhance hole transporting properties but also thermal properties. The para-linkage, **PF-p-In**, facilitates π-electron delocalization and thus has a lower optical band gap and a higher emission maximum than those of the meta linkage, **PF-m-In**. The electroluminescence devices based on **PF-p-In** and **PF-m-In** as the emissive layer show a similar maximum luminance but with different emissive colors of green and blue, respectively. The FET hole mobilities of **PF-p-In** and **PF-m-In** are 6.73×10^{-5} and 1.50×10^{-4} cm^2/V·s, respectively, which are significantly higher than that of polyfluorene. The present study demonstrates the electronic and optoelectronic properties of polyfluorene enhanced by incorporating hole transporting indolocarbazole with different linkages.

KEY WORDS: Functional Polymers / Polymer Synthesis / Light-Emitting Diodes / Field Effect Transistors / Fluorene / Indolocarbazole /

Conjugated polymers have been extensively studied for various electronic and optoelectronic devices, such as electroluminescence displays, photovoltaic cells, and field effect transistors.[1–5] Oligo- and polyfluorene as well as their derivatives are excellent candidates for optoelectronic applications because they exhibit high thermal/chemical stability, excellent fluorescence quantum yields, and solution processibility.[6,7] However, the relatively high ionization potential and low electron affinity of poly(9,9-dialkylfluorene) lead to poor carrier injection from the electrodes. Thus, limited electroluminescence (EL) efficiency and insignificant or no field effect mobility were reported in the literature.[8,9]

The electronic and optoelectronic properties of polyfluorene could be improved through the approaches of copolymer, blend, side chain modification, end-capping, or nanofiber and result in enhanced device characteristics.[8–17] For example, the copolymers of fluorene with hole transporting moieties of phenothiazine and phenoxazine led to enhanced EL characteristics[8] and field effect mobility,[9] respectively. The incorporation of acceptor and donor-acceptor-donor moiety into polyfluorene also successfully improved the EL or FET characteristics.[12–15] Indolocarbazole-based materials have emerged as new p-type organic semiconductors due to relatively high hole-transporting mobility and photo-oxidative stability. Relatively high hole mobilities of 0.2 and 0.02 cm^2 V^{-1} s^{-1} were reported for the indolo[3,2-b]carbazole[18–20] and polymer derivatives,[21–23] respectively. Hence, it would be of interest to explore the synthesis and properties of fluorene-indolocarbazole copolymers.

In this study, new alternating copolymers of 9,9-dihexylfluorene and 3,9- or 2,8-substituted di(2-ethylhexyl)-indolo-[3,2-b]carbazole were synthesized and characterized. The effects of indolocarbazole and its linkage position on the electronic, photoluminescence, and electrochemical properties of the synthesized copolymers were explored. Electroluminescence and field effect transistor devices based on the synthesized copolymers were also studied and compared with the parent polyfluorenes (**PF**). The present study suggests that the hole transporting property and device characteristics of polyfluorene are significantly improved by incorporating indolocarbazole.

EXPERIMENTAL

Reagents and Materials

1,4-Cyclohexanedione, 3-bromophenylhydrazine hydrochloride, 4-bromophenylhydrazine hydrochloride, 2-ethylhexylbromide, glacial acetic acid, sulfuric acid, 9,9-dihexylfluorene-2,7-bis(trimethyleneborate), tetrakis-(triphenylphosphine)-palladium(0), and potassium carbonate and trioctylmeth-ylammonium chloride (aliquat® 336) were purchased from Aldrich (Missouri, USA) or Acros (Geel, Belgium) and used without further purification. *N*,*N*-dimethyl-formamide (DMF), *N*,*N*-dimethylsulfoxide (DMSO) and ethanol (EtOH) were purchased from Tedia (Ohio, USA). All starting reagents and solvents were used in the reactions under nitrogen. 2,8-Dibromo-5,11-di(2′-ethylhexyl)-indolo[3,2-b]carbazole and 3,9-dibromo-5,11-di(2′-ethylhexyl)-indolo[3,2-b]carbazole were prepared according to the literature report.[23]

[1]Department of Chemical Engineering, National Taiwan University, Taipei, Taiwan 106
[2]Institute of Polymer Science and Engineering, National Taiwan University, Taipei, Taiwan 106
[3]Energy and Environmental Laboratories, Industrial Technology Research Institute, Hsinchu, Taiwan 310
*To whom correspondence should be addressed (Tel: +886-2-23628398, Fax: +886-2-23623040, E-mail: chenwc@ntu.edu.tw).

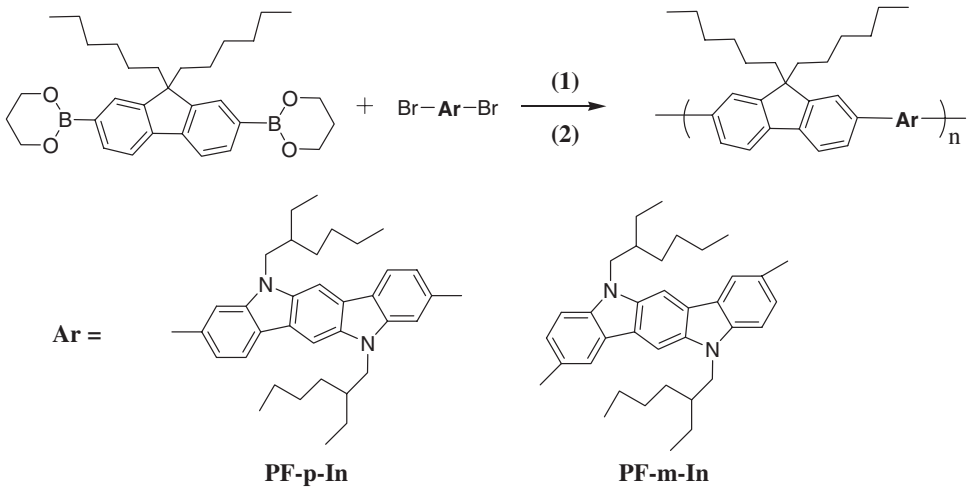

Synthetic routes :

(1) $Pd(PPh_3)_4$ / K_2CO_3 / Toluene

(2) Phenyl boronic acid / Bromobenzene

Scheme 1.

General Procedures of the Suzuki Coupling Polymerization

Syntheses of the copolymers were carried out using palladium-catalyzed Suzuki coupling polymerization, as shown in Scheme 1. 9,9-Dihexyl-fluorene-2,7-bis(trimethyleneborate), 2,8-dibromo-5,11-di(2′-ethylhexyl)-indolo[3,2-b]carbazole or 3,9-dibromo-5,11-di(2′-ethylhexyl)-indolo[3,2-b]carbazole), tetrakis(triphenylphosphine)palladium (0) (1 mol % with respect to diborate monomer), and several drops of aliquat® 336 were dissolved in toluene. To the reaction mixture, degassed aqueous 2 M K_2CO_3 (3.3 equiv. with respect to the diborate monomer) was added. The mixture was refluxed with vigorous stirring for 72 h under a nitrogen atmosphere. The end groups were capped by refluxing with phenyl boronic acid and bromobenzene (both 1.1 equiv. with respect to diborate monomer) for 12 h each. After end capped, the reaction mixture was cooled and poured into a mixed solvent of methanol and water. The precipitated product was dissolved into a small amount of THF and then re-precipitated into methanol to afford a crude polymer. The crude polymer was washed with acetone for 24 h to remove oligomers and catalyst residues.

Poly[2,7-(9,9′-dihexylfluorene)-*alt*-3,9-(5,11-di(2-ethylhexyl)-indolo[3,2-b]carbazole)] (PF-p-In). 9,9-Dihexylfluorene-2,7-bis(trimethyleneborate) (502 mg; 1 mmol) and 3,9-dibromo-5,11-di(2′-ethylhexyl)-indolo[3,2-b]carbazole (638 mg; 1 mmol) were dissolved in 10 mL of anhydrous toluene under nitrogen atmosphere. The final product, a yellow-green polymer with a yield of 560 mg (70.3%), was obtained after drying in vacuum at 80 °C. Anal. Calcd (wt %) for $(C_{58}H_{72}N_2)_n$: C, 87.16; H, 9.33; N, 3.51. Found: C, 85.03, H, 9.13, N, 3.32. FT/IR (KBr pellet, cm^{-1}): 2956 ($-CH_3$ stretching), 1465 ($-CH_2-$ bending). ^1H NMR (300 MHz, $CDCl_3$, ppm): 8.30 (2H); 8.04 (2H); 7.87 (2H); 7.78 (4H); 7.69 (2H); 7.59 (2H); 4.38 (4H); 2.29 (2H); 2.16 (4H); 1.35 (8H); 1.25 (4H); 1.13 (16H); 0.91 (10H); 0.78 (10H). GPC: M_n (the number-average molecular weight): 8800 and PDI (polydispersity index): 1.34.

Poly[2,7-(9,9′-dihexylfluorene)-*alt*-2,8-(5,11-di(2-ethylhexyl)-indolo[3,2-b]carbazole)] (PF-m-In). 9,9-Dihexylfluorene-2,7-bis(trimethyleneborate) (502 mg; 1 mmol) and 2,8-dibromo-5,11-di(2′-ethylhexyl)-indolo[3,2-b]carbazole (638 mg; 1 mmol) were dissolved in 10 mL of anhydrous toluene under nitrogen for 10 min. The final product, a yellow-green polymer with a yield of 586 mg (73.5%), was obtained after drying in vacuum at 80 °C. Anal. Calcd (wt %) for $(C_{58}H_{72}N_2)_n$: C, 87.16; H, 9.33; N, 3.51. Found: C, 86.88, H: 8.40; N, 3.30. FT/IR (KBr pellet, cm^{-1}): 2952 ($-CH_3$ stretching), 1463 ($-CH_2-$ bending). ^1H NMR (300 MHz, $CDCl_3$, ppm): 8.48 (2H); 8.10 (2H); 7.83–7.78 (6H); 7.55 (2H); 7.49 (2H); 4.34 (4H); 2.25 (2H); 2.11 (4H); 1.34 (8H); 1.23 (4H); 1.13 (16H); 0.92 (10H); 0.78 (10H). GPC: M_n (the number-average molecular weight): 5700 and PDI (polydispersity index): 2.07.

Characterization Methods

^1H NMR spectra were measured on a Bruker AV 500 MHz spectrometer using $CDCl_3$ as the solvent and tetramethylsilane as internal reference. Fourier transform infrared spectrometer was measured in a Perkin Elmer FT/IR spectrometer 100. Weight-average molecular weights and number-average molecular weights were obtained *via* size exclusion chromatography (SEC) on the basis of polystyrene calibration using a Water 2410 apparatus and tetrahydrofuran (THF) as the eluent. Elemental analyses were run in a Heraeus Vario-III analyzer.

Thermogravimetric analysis (TGA) was conducted with a pyris 1 TGA. Experiments were carried out on 3–6 mg samples heated under nitrogen atmosphere at a heating rate of 20 °C/min. Differential scanning calorimetry (DSC) was performed on a TA instrument DSC-910S differential scanning calorim-

eter under nitrogen atmosphere at a heating rate of 10 °C/min. UV-visible absorption and photoluminescence (PL) spectra were obtained on a Jasco model UV/VIS/NIR V-570 spectrometer and Fluorolog-3 spectrofluorometer (Jobin Yvon), respectively. For the solution spectra, polymers were dissolved in THF (*ca.* 10^{-6} M) and then put in a quartz cell for measurement. For the thin film spectra, polymers were first dissolved in THF (1 wt %) and then spin-coated on glass substrate at 1000 rpm for 30 s. Then, the thin films were dried at 60 °C under vacuum. Films used for the PL efficiency measurement were drop-coated from THF solution onto quartz substrates (*ca.* 1 wt %). PL efficiencies of the films on quartz substrates were measured by fluorolog 3. The electrochemical properties of the polymer films were investigated on a Princeton Applied Research Model 273A Potentiostat/Galvanostat with a 0.1 M acetonitrile solution containing tetrabutylammonium tetrafluoroborate ($TBABF_4$) as the electrolyte. Platinum wire and rod-tip electrodes were used as counter and working electrodes respectively. Silver/silver ion (Ag in 0.1 M $AgNO_3$ in the supporting electrolyte solutions) was used as a reference electrode. A 3 wt % solution of a polymer in THF was used to prepare the polymer film on the Pt rod-tip electrode. Then, the cyclic voltammetry of films was performed on a three-electrode cell.

Polymer Light-Emitting Devices (LED)

The polymer LED devices were fabricated in the configuration of ITO/poly(ethylene dioxythiophene):poly(styrenesulfonate) (PEDOT:PSS) (50–60 nm)/light-emitting layer (70–80 nm)/Ca (10 nm)/Ag (100 nm). Onto the ITO glass a layer of poly(ethylene dioxythiophene):poly(styrene sulfonate) (PEDOT:PSS), 50–60 nm thick (probed by Alpha-Step® 500 Surface Profiler), was formed by spin-coating from its aqueous solution (Baytron P 8000, Bayer) to enhance the hole injection and the smoothness between layers. The light-emitting layer was spin-coated on top of the PEDOT:PSS layer from the corresponding filtered toluene solution (1.5 wt %) and also dried under vacuum. Under a base pressure below 2×10^{-6} Torr, a layer of Ca (10 nm) was vacuum deposited as cathode and a thick layer of Ag (100 nm) was deposited subsequently as the protecting layer. The current-voltage-luminance characteristics were measured using a computerized Keithley 2400 source meter and Konica-Minolta Chroma Meter CS-100A. The EL spectrum of device was recorded on Fluorolog-3 spectrofluorometer (Jobin Yvon).

Polymer Field Effect Transistors

The field effect transistor was fabricated from the **PF-p-In** or **PF-m-In** with a bottom-contact configuration on the p-doped silicon wafers. A thermally grown 200 nm SiO_2 used as the gate dielectric with a capacitance of 17 nF/cm^2. Aluminum was used to create a common bottom-gate electrode. The source/drain regions were defined by a 10 nm thick chromium adhesion layer and a 100 nm thick gold contact electrode through a regular shadow mask, and the channel length (L) and width (W) were 25 and 500 (or 1000) μm, respectively. Afterward, the substrate was modified with octyltrichlorosilane (OTS) as silane coupling agents. In order to fabricate good quality thin films, **PF-p-In** and **PF-m-In** were dissolved in toluene, respectively. The 0.5 wt % polymer solutions were filtered through 0.20 μm pore size of PTFE membrane syringe filters. The solutions were then spin-coated at a speed rate of 1000 rpm for 60 s onto the OTS modified SiO_2/Si substrate and heated at 60 °C for 12 h in N_2. Output and transfer characteristics of the FET devices were measured using Keithley 4200 semiconductor parametric analyzer in ambient atmosphere.

RESULTS AND DISCUSSION

Polymer Structures

Figure 1 shows the ^{1}H NMR spectrum of **PF-p-In** in $CDCl_3$. The peaks at 7.53–8.30 ppm are assigned to the phenylene protons of indolocabazole and fluorene backbone. The peaks at 2.14 and 4.38 ppm are assigned to the methylene protons adjacent to fluorene 9-position and indolocarbazole N-position, respectively. The ^{1}H NMR spectrum of **PF-m-In** also agrees well with the proposed structure, as shown in the supporting information (Figure S1). The FT/IR spectra of **PF-p-In** and **PF-m-In** exhibit the expected CH_2, CH_3, and C-N vibration band, as exhibited in Figure S2 of the supporting information. The difference between the experimental and theoretical carbon contents from the elemental analysis is probably due to the end group effect from the low molecular weights of the prepared polymers. The two copolymers are soluble in common solvents, such as chloroform and THF at room temperature. The number-average molecular weights and polydispersity index (M_n, PDI) of **PF-p-In** and **PF-m-In** are (8800, 1.34), and (5700, 2.07), respectively. The above results suggest that the successful preparation of the target copolymers.

Thermal Properties

Figure 2 shows the DSC curves of **PF-p-In** and **PF-m-In**, in which the TGA curves are shown in the insert figure. The thermal decomposition temperatures (T_d) of **PF-p-In** and **PF-m-In** under nitrogen atmospheres are 417 and 449 °C, respectively. The char yield is more than 53% at 800 °C under nitrogen. The glass transition temperatures (T_g) of **PF-p-In** and **PF-m-In** are 109 and 156 °C, respectively. Note that the T_d and T_g of the polyfluorene (**PF**) homopolymer are 409 and 67 °C.[13] The higher thermal stability of the **PF-p-In** and **PF-m-In** than that of **PF** is due to the incorporation of ladder-like indolocarbazole backbone into polymer structure. The higher T_g of the **PF-m-In** than that of **PF-p-In** could be due to the less rotational freedom of the former because of the steric hindrance on the meta-position structure.[24]

Electronic and Optoelectronic Properties

The photophysical properties of **PF-p-In** and **PF-m-In** in solutions and solid state films are summarized in Table I. Figure 3 shows the normalized UV–vis absorption and photoluminescence spectra of **PF-p-In** and **PF-m-In** in solid state

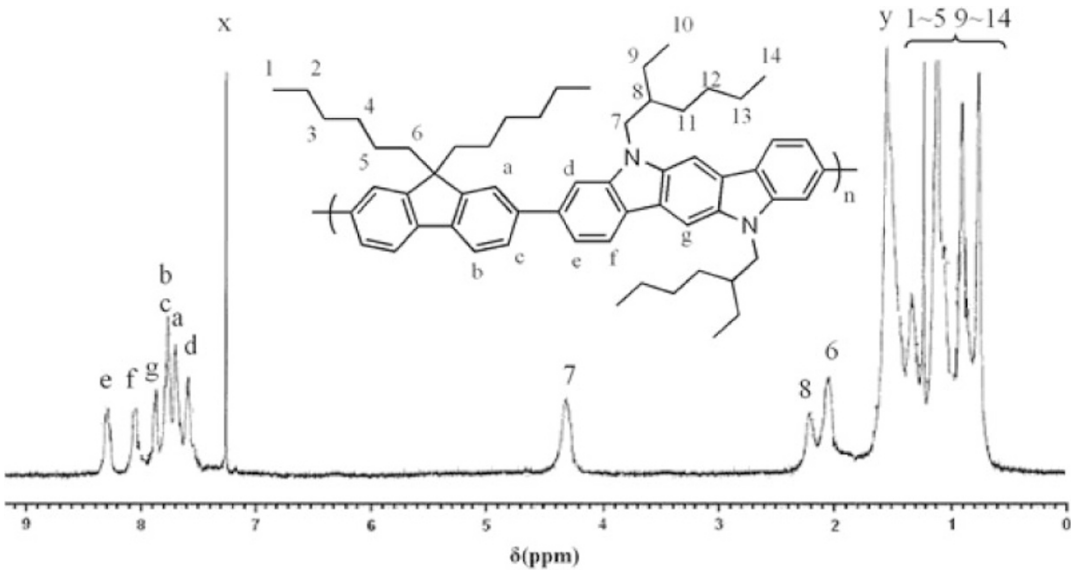

Figure 1. ^{1}H NMR spectra of **PF-p-In** in $CDCl_3$. The labels of x and y are $CDCl_3$ and H_2O, respectively.

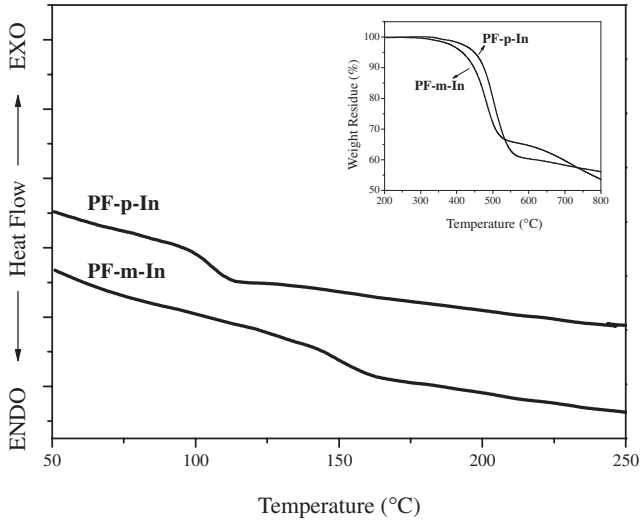

Figure 2. DSC curves of **PF-p-In** and **PF-m-In** at a heating rate of 20 °C/min under a nitrogen atmosphere. The insert figure shows TGA curves of **PF-p-In** and **PF-m-In** at a heating rate of 20 °C/min under a nitrogen atmosphere.

films. The normalized PL and UV–vis spectra are obtained through the ratio of absorption or fluorescence intensity at different wavelength to the maximum intensity. The optical absorption maxima ($\lambda_{abs,\,max}$) of **PF-p-In** and **PF-m-In** in solid state films are 391 and 363 nm, respectively, while the corresponding optical band gaps (eV) estimated from the absorption edges are 2.78 and 2.87 eV, respectively. The solution spectra of the above two polymers also show a similar trend on the linkage effect of the photophysical properties. The para-linkage, **PF-p-In**, facilitates the π-electron delocalization and results in a lower band gap than the meta-linkage, **PF-m-In**. The extended tails and/or shoulders near the absorption edges of **PF-p-In** and **PF-m-In** suggest stronger inter-chain interaction as compared to the parent **PF**. The optical band gaps of **PF-p-In** and **PF-m-In** are smaller than that of polyfluorene (**PF**) with 2.95 eV, due to the incorporation of the highly conjugated indolocarbazole.

The higher emission maximum ($\lambda_{PL,\,max}$) of **PF-p-In** at 500 nm than that of **PF-m-In** with 468 nm in Figure 3 is resulted from the lower band gap of the former due to the para-linkage. The solution photoluminescence spectra also show a similar trend. Both polymers have a high emission maxima than those of **PF** with (424 and 445 nm) reported previously,[13] due to the lower band gap of the former.

Figure 4 shows the cyclic voltammograms of **PF-p-In** and **PF-m-In** and the corresponding electrochemical results are listed in Table I. The onset oxidation (E_{onset}) of **PF-p-In**

Table I. Optical and Electrochemical Properties of **PF-p-In** and **PF-m-In**

Polymer	Solution (THF)		Film		Oxidation (V) (v.s. Ag/AgCl)		HOMO (eV)[d]	LUMO (eV)[e]
	$\lambda_{abs,\,max}$ (nm)	$\lambda_{PL,\,max}$ (nm)	$\lambda_{abs,\,max}$ (nm)	Eg^{opt} (eV)[a]	Quantum yield (%)	$E_{1/2}$ (V)[b]	E_{onset} (V)[c]		
PF-p-In	392	457, 487	391	2.78	33	0.87	0.74	−5.10	−2.32
PF-m-In	357	437, 463	363	2.87	29	0.93	0.87	−5.23	−2.36

[a]Optical band gap (E_g^{opt}) = 1240/λ_{onset} (nm). [b]Average potential of the redox couple peaks (V *vs.* Ag/AgCl) in CH_3CN. [c]Onset potentials (V *vs.* Ag/AgCl) in CH_3CN. [d]The HOMO energy levels were calculated from cyclic voltammetry and were referenced to ferrocene (4.8 eV). [e]No reduction potential was observed in the CV. Thus, the LUMO level was estimated by the following relation: $E_{LUMO} = E_{HOMO} + E_g^{opt}$.

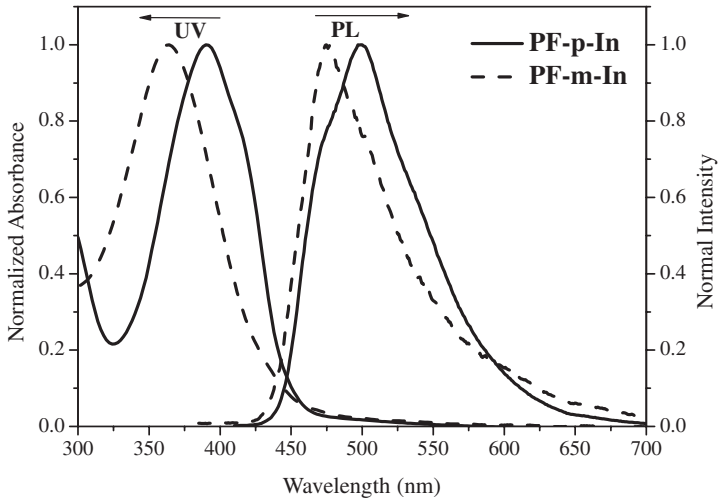

Figure 3. UV–vis absorption and photoluminescence spectra of **PF-p-In** and **PF-m-In** films on quartz substrates.

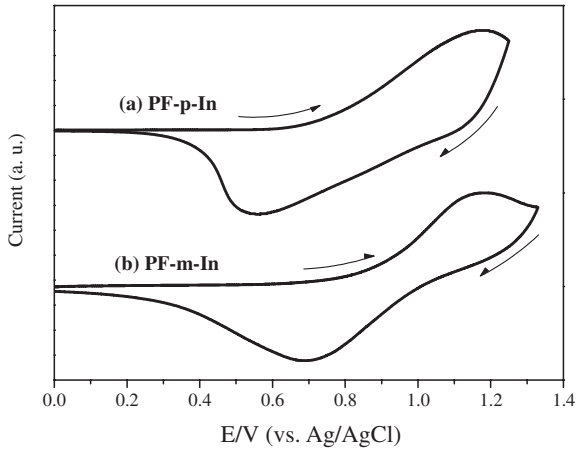

Figure 4. Cyclic voltammograms of (a) **PF-p-In** and (b) **PF-m-In** at scan rate = 100 mV/s. The films in a 0.1 M acetonitrile solution containing tetrabutylammonium tetrafluoroborate ($TBABF_4$) as the electrolyte. Note that anodic current is taken as positive and positive potential is plotted to the right.

is 0.74 V *vs* Ag/AgCl. The ferrocene/ferrocenium (Fc/Fc^+) redox standard $E_{1/2}$ is 0.44 V *vs* Ag/AgCl in CH_3CN. Assuming that the energy for the Fc/Fc^+ standard is 4.8 eV with respect to the zero vacuum level,[25] the ionization potential (IP) for **PF-p-In** is estimated to be 5.10 eV ($IP = E_{onset} - 0.44 + 4.8$). Thus, the corresponding HOMO level of **PF-p-In** is −5.10 eV from the relation of HOMO = −IP. Similarly, the HOMO level of **PF-m-In** is estimated to be −5.23 eV. The HOMO level of the **PF** reported previously[13] is at −5.39 eV. It suggests that the hole transporting property of **PF** is improved by incorporating indolocabazole. The lower HOMO energy level of the **PF-p-In** than that of **PF-m-In** probably results from the better π electron delocalization of the former.

Electroluminescence Properties of LED Devices

The LED devices with the studied copolymers as emissive layers were fabricated with configuration of ITO/PEDOT:PSS/emissive polymer/Ca/Ag. The emission characteristics of the above devices are listed in Table II. Figure 5 shows the EL spectra of **PF-p-In** and **PF-m-In** measured at maximum luminance yield. As shown in the Figure 5, the emission characteristics of **PF-p-In** and **PF-m-In** are quite different because of the different linking position between fluorene and indolocarbazole. The emission maxima of **PF-p-In** and **PF-m-In** are 498 and 467 nm, respectively. The blue-shifted EL spectrum of **PF-m-In** with respect to **PF-p-In** is resulted from the larger energy band gap of **PF-m-In**, since the meta linkage has a shorter π-conjugation length. It suggests that the emission color could be tuned through different linkages.

The relatively low turn-on voltages (5–6 V) of **PF-p-In** and **PF-m-In** are due to the higher HOMO energy levels and the better hole transporting properties by incorporating indolocarbazole into **PF**. Note that the turn-on voltage of the **PF** device is around 10 V.[13] The **PF-p-In** and **PF-m-In** device have maximum luminance intensities of 219 and 181 cd/m^2, respectively. It indicates that the maximum luminance inten-

Table II. Electroluminescence characteristics of **PF-p-In** and **PF-m-In**

Polymer	λ_{max}^{EL} (nm)	Bias (V)	Current density[a] (mA/cm^2)	Luminance (cd/m^2)	Luminance yield (cd/A)	Chromaticity Coordinate[b]	
						x	y
PF-p-In	498	11	386.1	219	0.057	0.241	0.426
PF-m-In	446*, 467	12	290.6	181	0.062	0.191	0.229

Device Structure: ITO/PEDOT:PSS/Emissive Layer/Ca/Ag. Measured at maximum luminance yield. [a]Active area is 0.1256 cm^2. [b]The commission Internationale de L'Eclairage (CIE) 1931 coordinates. *Emission shoulder.

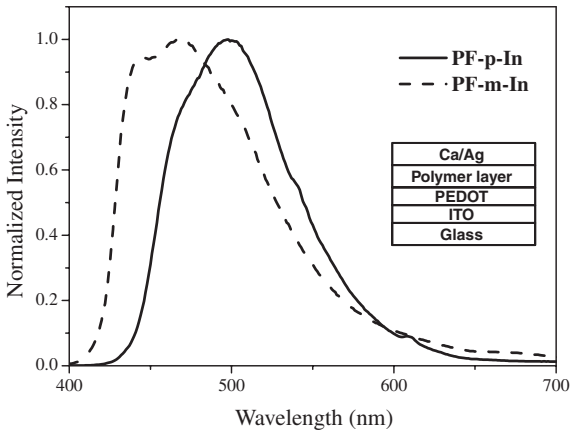

Figure 5. Electroluminescence spectra of **PF-p-In** and **PF-m-In** measured at maximum luminance yield based on the device structure of ITO/PEDOT:PSS/emissive polymer/Ca/Ag.

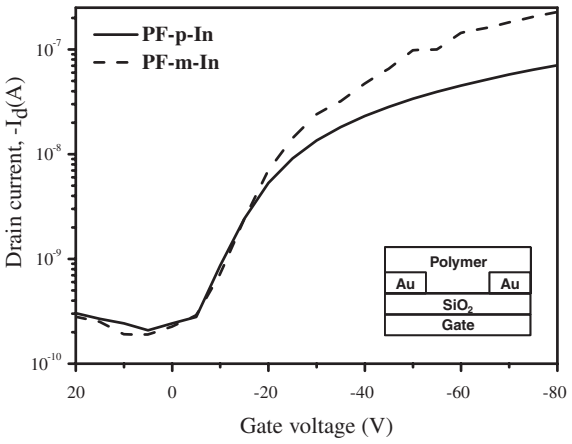

Figure 6. The transfer characteristics (drain current (I_d) versus drain voltage (V_d) at various gate voltage (V_g)) of **PF-p-In** and **PF-m-In** based field effect transistors.

sities of the devices are not obviously affected by the different linkages (para- or meta-) between fluorene and indolocarbazole except the emission color. The commission Internationale de L'Eclairage (CIE) 1931 coordinates of the EL devices with **PF-p-In**, and **PF-m-In** measured at maximum luminance yield are (0.241, 0.426) and (0.191, 0.229), with the corresponding emissive colors of green and blue. These results suggest that the color tuning and enhancement of device performances could be accomplished with incorporating the hole-transporting indolocarbazole into polyfluorene.

Field-effect Transistor (FET) Characteristics

Figure 6 exhibits typical p-channel transfer characteristics (drain current (I_d) versus drain voltage (V_d) at various gate voltage (V_g)) of **PF-p-In** and **PF-m-In** FETs. In the saturation region ($V_d > V_g - V_t$), where V_t is the threshold voltage, I_d can be described by equation (1):[26]

$$I_d = \frac{WC_o\mu_h}{2L}(V_g - V_t)^2 \quad (1)$$

Where μ_h is the hole mobility, W is the channel width, L is the channel length, and C_o is the capacitance of the gate insulator per unit area, respectively. The saturation region mobility of the studied polymers is calculated from the transfer characteristics of FETs. The hole mobilities of **PF-p-In** and **PF-m-In** estimated from Figure 6 and equation (1) are 6.73×10^{-5} and 1.50×10^{-4} $cm^2/V{\cdot}s$, respectively. The on-off ratios are 7×10^2 and 4×10^2. The hole mobility of **PF-m-In** is clearly higher than **PF-p-In**. **PF-m-In** with the 2,8-linkages could provide more resonance stabilization to the ammonium cation, and aid the process of charge transport.[18,21] However, such resonance stabilization could not be supplied by **PF-p-In**. Therefore, the performance of charge transporting characteristics of **PF-m-In** is better than that of **PF-p-In**. No FET hole mobility is observed for **PF**. It suggests that the incorporation of indolocarbazole segments into polyfluorene could enhance charge carrier mobility. Besides, the fluorene-indolocarbazole copolymer based FET devices have the threshold voltage about −3 V. It indicates that the energy barrier of injection between Au and polymers is small since the HOMO energy levels of the polymers are very close to the working function of Au (5.1 eV).

CONCLUSIONS

The charge transporting characteristics and electroluminescence properties of two new fluorene-indolocarbazole alternating copolymers with different linkage position are reported in this study. The para-linkage **PF-p-In** has a low optical band gap and higher emission maximum than those of the meta-linkage **PF-m-In**. The FET hole mobilities of **PF-p-In** and **PF-m-In** are significantly higher than that of polyfluorene. Besides, the **PF-m-In** could provide sufficient resonance stabilization and thus higher FET performance than **PF-p-In**. The present study exhibits the significance of the indolocarbazole moiety and backbone linkages (2,8- or 3,9-linkages) on the electronic and optoelectronic properties of the fluorene-indolocarbazole copolymers.

Acknowledgment. The financial support from National Science council of Taiwan, Ministry of Education, and Ministry of Economics Affairs are highly appreciated.

Electronic Supporting Information Available: Figures S1 and S2. These materials are available *via.* the Internet at http://www.spsj.or.jp/c5/pj/pj.htm.

Received: September 14, 2007
Accepted: December 3, 2007
Published: January 17, 2008

REFERENCES

1. A. Kraft, A. C. Grimsdale, and A. B. Holmes, *Angew. Chem. Int. Ed.*, **37**, 402 (1998).
2. L. L. Chua, J. Zaumseil, J. F. Chang, E. C.-W. Ou, P. K.-H. Ho, H. Sirringhaus, and R. H. Friend, *Nature*, **434**, 194 (2005).
3. G. Yu, J. Gao, J. C. Hummelen, F. Wudl, and A. J . Heeger, *Science*,

270, 1789 (1995).
4. G. Li, V. Shrotriya, J. Huang, Y. Yao, T. Moriarty, K. Emery, and Y. Yang, *Nature Mater.*, **4**, 864 (2005).
5. S. Seki and S. Tagawa, *Polym. J.*, **39**, 277 (2007).
6. U. Scherf and E. J. W. List, *Adv. Mater.*, **14**, 477 (2002).
7. D. Neher, *Macromol. Rapid Commun.*, **22**, 1365 (2001).
8. A. P. Kulkarni, X. Kong, and S. A. Jenekhe, *Macromolecules*, **39**, 8699 (2006).
9. Y. Zhu, A. Babel, and S. A. Jenekhe, *Macromolecules*, **38**, 7983 (2005).
10. S. Xiao, M. Nguyen, X. Gong, Y. Cao, H. Wu, D. Moses, and A. J. Heeger, *Adv. Funct. Mater.*, **13**, 25 (2003).
11. W. J. Lin, W. C. Chen, W.-C. Wu, Y. H. Niu, and A. K. Y. Jen, *Macromolecules*, **37**, 2335 (2004).
12. W. C. Wu and W. C. Chen, *J. Polym. Res.*, **13**, 441 (2006).
13. W. C. Wu, C. L. Liu, and W. C. Chen, *Polymer*, **47**, 527 (2006).
14. Q. Peng, J. B. Peng, E. T. Kang, K. G. Neoh, and Y. Cao, *Macromolecules*, **38**, 7292 (2005).
15. W. Y. Lee, K. F. Chang, T. F. Wang, C. C. Chueh, W. C. Chen, C. S. Tuan, and J. L. Lin, *Macromol. Chem. Phys.*, **208**, 1919 (2007).
16. C. C. Kuo, J. H. Lin, and W. C. Chen, *Macromolecules*, **40**, 6959 (2007).
17. K. Takagi, K. Saiki, K. Mori, Y. Yuki, and M. Suzuki, *Polym. J.*, **39**, 813 (2007).
18. Y. Li, Y. Wu, S. Gardner, and B. S. Ong, *Adv. Mater.*, **17**, 849 (2005).
19. Y. Wu, Y. Li, S. Gardner, and B. S. Ong, *J. Am. Chem. Soc.*, **127**, 614 (2005).
20. P.-L. Boudreau, S. Wakim, S. N. Blouin, M. Simard, C. Tessier, Y. Tao, and M. Leclerc, *J. Am. Chem. Soc.*, **129**, 9125 (2007).
21. Y. Li, Y. Wu, and B. S. Ong, *Macromolecules*, **39**, 6521 (2006).
22. N. Blouin, A. Michaud, S. Wakim, P.-L. T. Boudrealt, M. Leclerc, B. Vercelli, S. Zecchin, and G. Zotti, *Macromol. Chem. Phys.*, **207**, 166 (2006).
23. N. Blouin, M. Leclerc, B. Vercelli, S. Zecchin, and G. Zotti, *Macromol. Chem. Phys.*, **207**, 175 (2006).
24. Y. K. Jung, J. Lee, S. K. Lee, H.-J. Cho, and H.-K. Shim, *J. Polym. Sci., Part A: Polym. Chem.*, **44**, 4611 (2006).
25. G. S. Liou, S. H. Hsiao, W. C. Chen, and H.-J. Yen, *Macromolecules*, **39**, 6036 (2006).
26. Z. Bao, A. Dodabalapur, and A. J. Lovinger, *Appl. Phys. Lett.*, **69**, 4108 (1996).